Molecular Cell, Volume *51*

Supplemental Information

Structural Architecture of the CARMA1/Bcl10/MALT1 Signalosome: Nucleation-Induced Filamentous Assembly

Qi Qiao, Chenghua Yang, Chao Zheng, Lorena Fontán, Liron David, Xiong Yu, Clay Bracken, Monica Rosen, Ari Melnick, Edward H. Egelman, and Hao Wu

Inventory of Supplemental Information

SUPPLEMENTAL FIGURES

SUPPLEMENTAL TABLES

SUPPLEMENTAL EXPERIMENTAL PROCEDURES

Cell Transfection and Coimmunoprecipitation

Crystallization and Structure Determination

NMR Spectroscopy and Structure Calculations

Luciferase Assays

TRAF6 Knockdown

SUPPLEMENTAL REFERENCES

Supplemental Information

SUPPLEMENTAL FIGURES

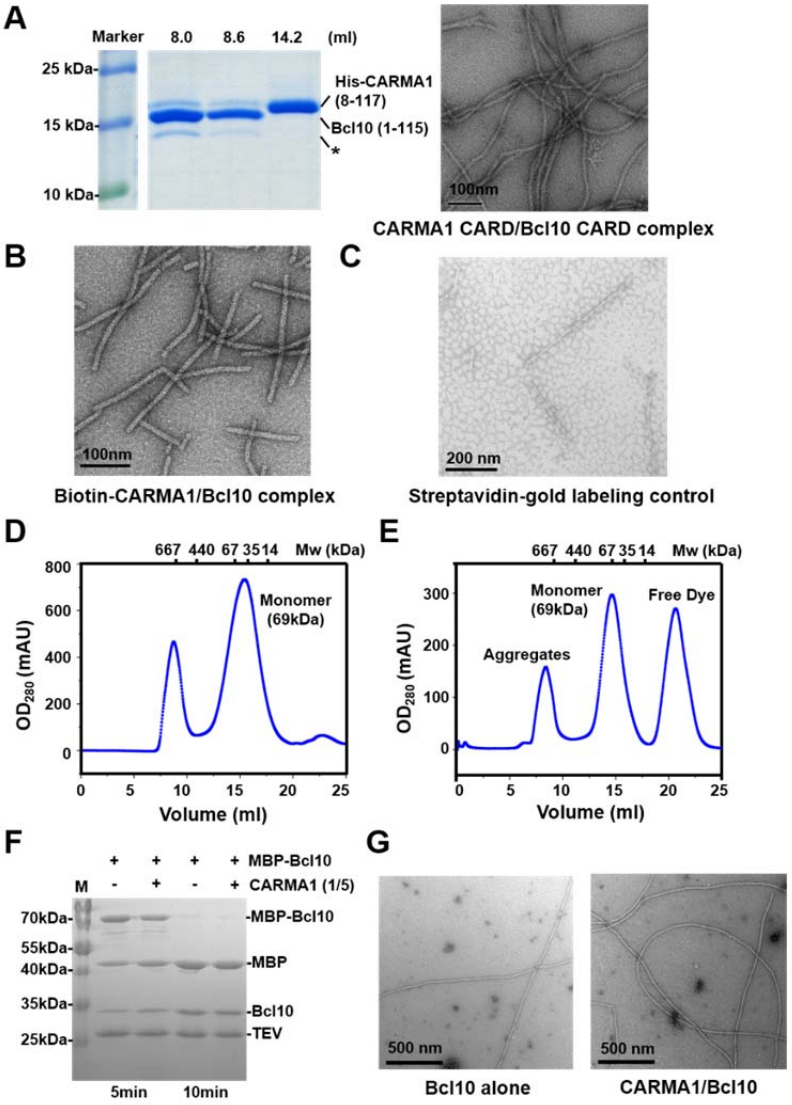

Figure S1. The CARMA1/Bcl10 Complex is Filamentous with End Localization of CARMA1, Related to Figure 1

(A) CARMA1 CARD and Bcl10 CARD form a complex upon co-expression. Left: SDS-PAGE gel of the complex fractions (8.0 and 8.6 ml) and the excess CARMA1 fraction (14.2 ml) from a Superdex 200 10/300 GL column. *: a contaminant. Right: an EM image of the negatively stained complex.

(B) An EM image of biotinylated CARMA1/Bcl10 filaments.

(C) An EM image of the negative control of streptavidin-gold labeling using non-biotinylated CARMA1/Bcl10 complex.

(D) Purification of MBP-Bcl10 C29A/C57A double mutant, showing the prominent monomeric peak.

(E) Purification of Alexa-488 labeled MBP-Bcl10 C29A/C57A double mutant using Superdex 200 10/300 GL. Monomeric peak fractions were collected for fluorescence polarization assays.

(F) SDS-PAGE gel showing the time course of TEV treatment of MBP-Bcl10 C29A/C57A double mutant for removal of the MBP tag. The reactions were carried out in the absence and presence of 1/5 molar ratio of CARMA1.

(G) EM images of Bcl10 alone and CARMA1/Bcl10 complex filaments generated from *in vitro* polymerization assays.

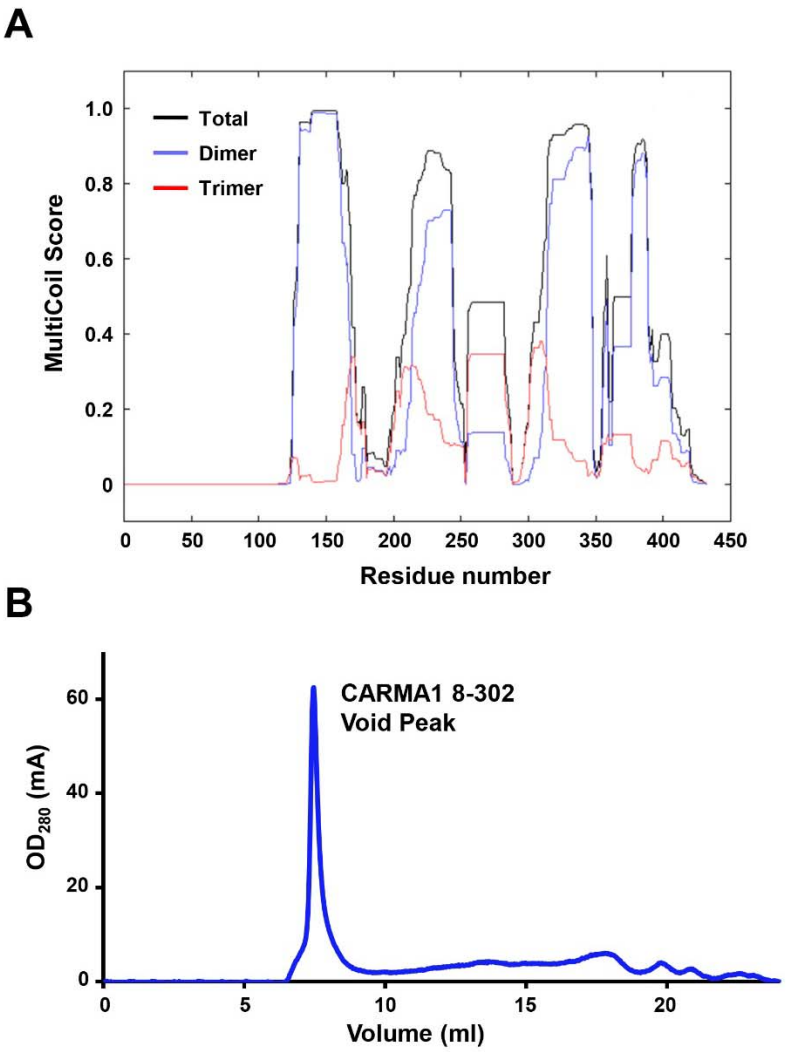

Figure S2. Prediction of coiled coil structures by MultiCoil (Wolf et al., 1997), Related to Figure 2.
(A) Approximate four potential coiled coil regions in CARMA1 are shown, around 120-175, 200-300 and 300-350, and 350-440.
(B) Gel filtration profile of CARMA1 (8-302) from a Superose 6 column showed a major void peak.

.

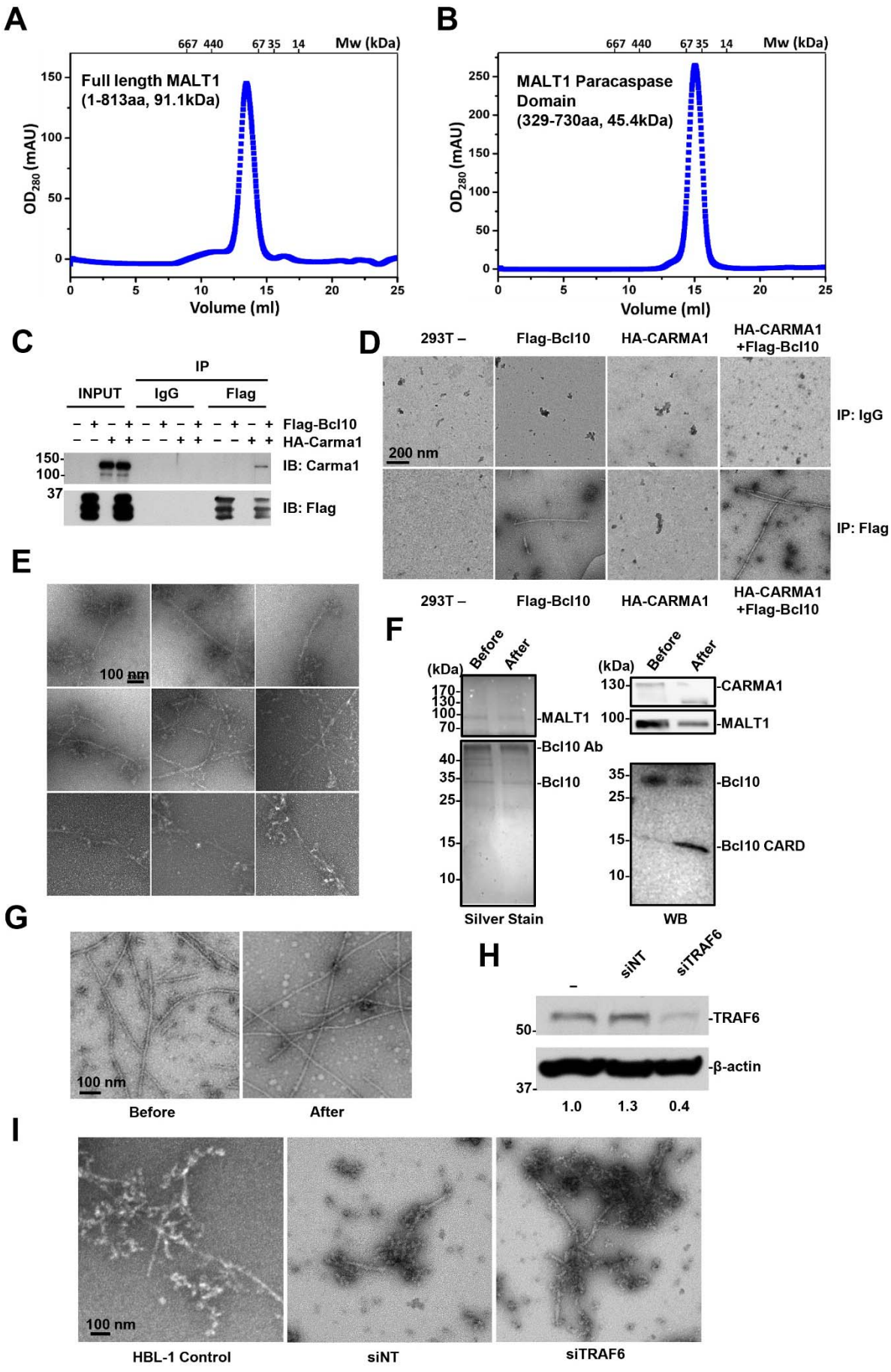
A
667 440 67 35 14 Mw (kDa)
Full length MALT1
(1-813aa, 91.1kDa)
OD280 (mAU)
Volume (ml)
B
667 440 67 35 14 Mw (kDa)
MALT1 Paracaspase
Domain
(329-730aa, 45.4kDa)
OD280 (mAU)
Volume (ml)
C
IP
INPUT
IgG
Flag
Flag-Bcl10
HA-Carma1
IB: Carma1
IB: Flag
D
293T –
Flag-Bcl10
HA-CARMA1
HA-CARMA1
+Flag-Bcl10
200 nm
IP: IgG
IP: Flag
E
100 nm
F
(kDa)
Before
After
MALT1
Bcl10 Ab
Bcl10
Silver Stain
CARMA1
MALT1
Bcl10
Bcl10 CARD
WB
G
100 nm
Before
After
H
siNT
siTRAF6
TRAF6
β-actin
1.0
1.3
0.4
I
100 nm
HBL-1 Control
siNT
siTRAF6

Figure S3. CBM Complexes *in Vitro* and in Cells, Related to Figure 3

(A) Gel filtration profile of insect cell expressed full-length MALT1.
(B) Gel filtration profile of *E. coli* expressed MALT1 paracaspase domain.
(C) Western blot of immunoprecipitation controls by isotype IgG and single transfections.
(D) Immunoprecipitated controls under EM.
(E) Additional EM images of endogenous CBM complex upon proteolysis.
(F) Silver stain and Western blot (WB) of endogenous immunoprecipitated sample before and after proteolysis.
(G) *In vitro* reconstituted Bcl10 filaments before and after proteolysis treatment.
(H) TRAF6 knockdown in HBL-1 cells by siRNA. siNT: control siRNA.
(I) Anti-Bcl10 immunoprecipitated samples from TRAF6 knockdown cells showed similar morphology with control HBL-1 and siNT samples.

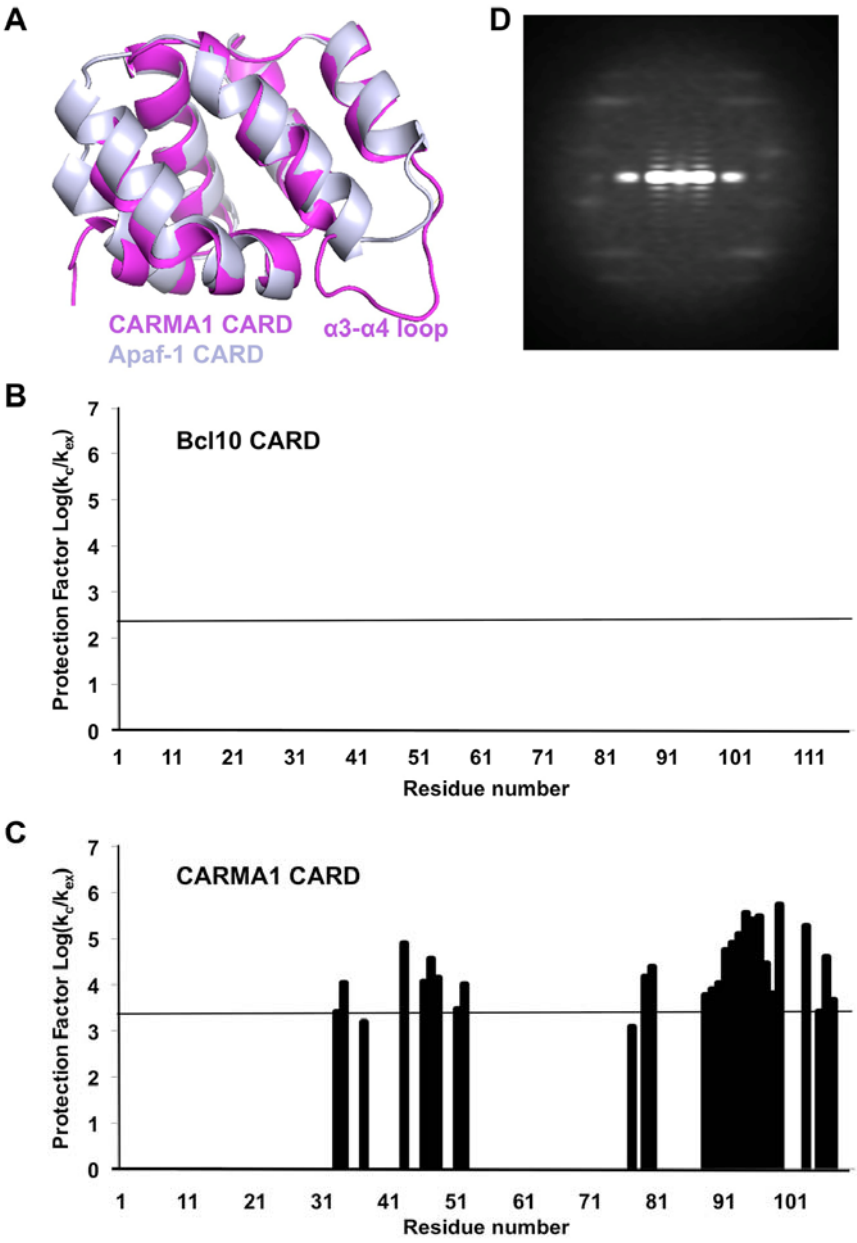

Figure S4. EM Structure of the Bcl10 Filament, Related to Figure 4

(A) Superposition between CARMA1 (magenta) and Apaf-1 (light purple) CARDs, showing the difference at the α3- α4 loop.

(B) Hydrogen protection factor for Bcl10 CARD, measured as the ratio between the random coil hydrogen exchange rate (k_c), which varies with sequence, and the measurable exchange rate (k_{ex}) observable at 310K and pH 7.0. Based on the sequence, pH and temperature conditions, the minimum intrinsic protection factors ($\log[k_c/k_{ex}]$) necessary for observing a signal within the experimental dead time for Bcl10 is 2.3. Bcl10 is fully exchanged within the dead time of the experiment.

(C) Hydrogen protection factor for CARMA1 CARD. Based on the sequence, pH and temperature conditions, the minimum intrinsic protection factors ($\log[k_c/k_{ex}]$) necessary for observing a signal within the experimental dead time for CARMA1 is 3.3. Many residues are protected within the dead time of the experiment.

(D) An averaged power spectrum of the CARMA1/Bcl10 complex filament.

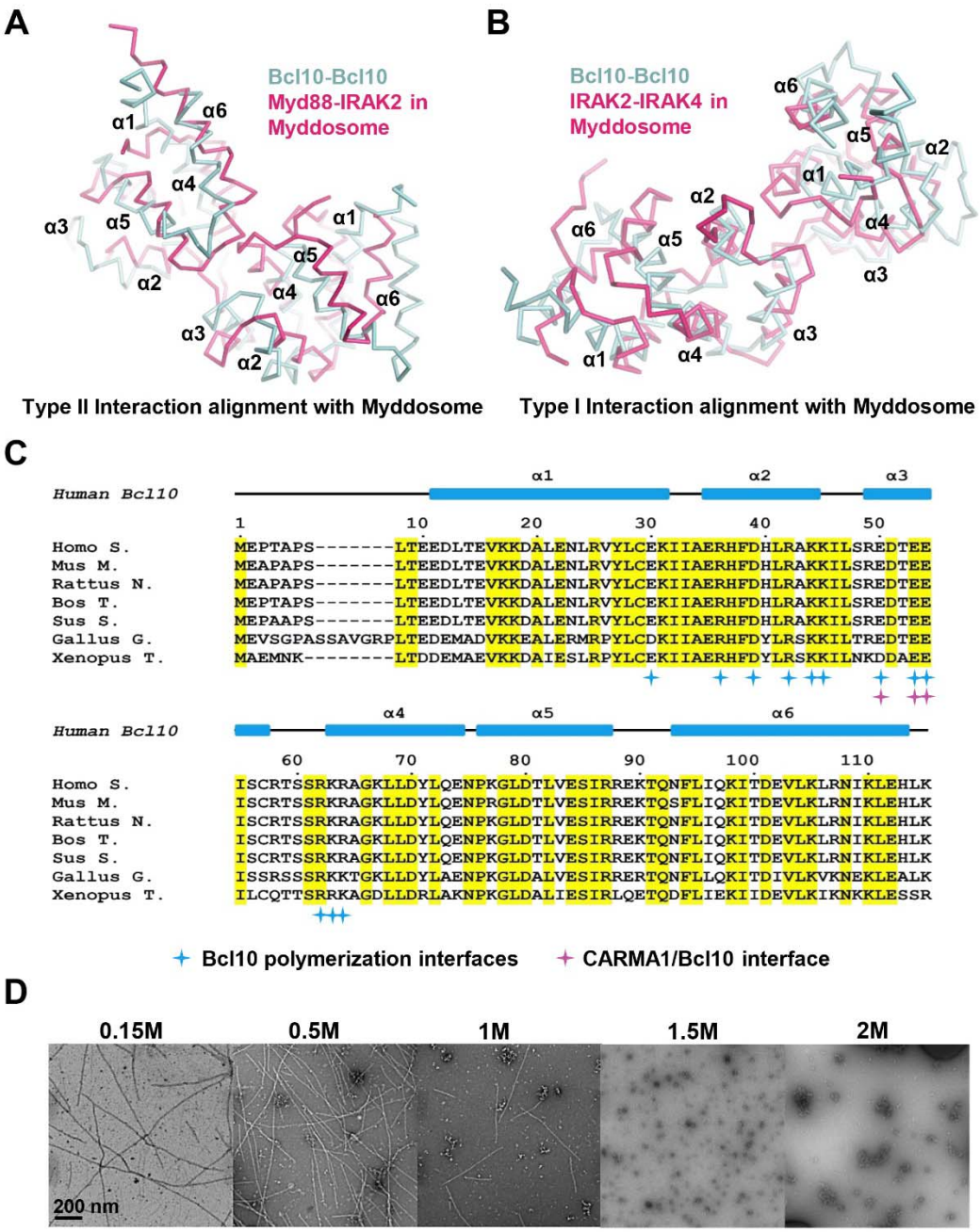

Figure S5. Detailed Interactions in the Bcl10 Filament, Related to Figure 5

(A) Structure alignment between the intrahelix type II interaction (cyan) and a type II interaction in Myddosome structure (magenta, PDB code: 3MOP) (Lin et al., 2010).

(B) Structure alignment between the interhelix type I interaction (cyan) and a type I interaction in the Myddosome (gray) (Lin et al., 2010).

(C) Sequence alignment of Bcl10 among different species. Residues involved in Bcl10 polymerization (cyan star) and CARMA1 interaction (magenta star) are labeled. Conserved residues between species were highlighted in bright yellow.

(D) EM images of Bcl10 polymerization under different salt concentrations.

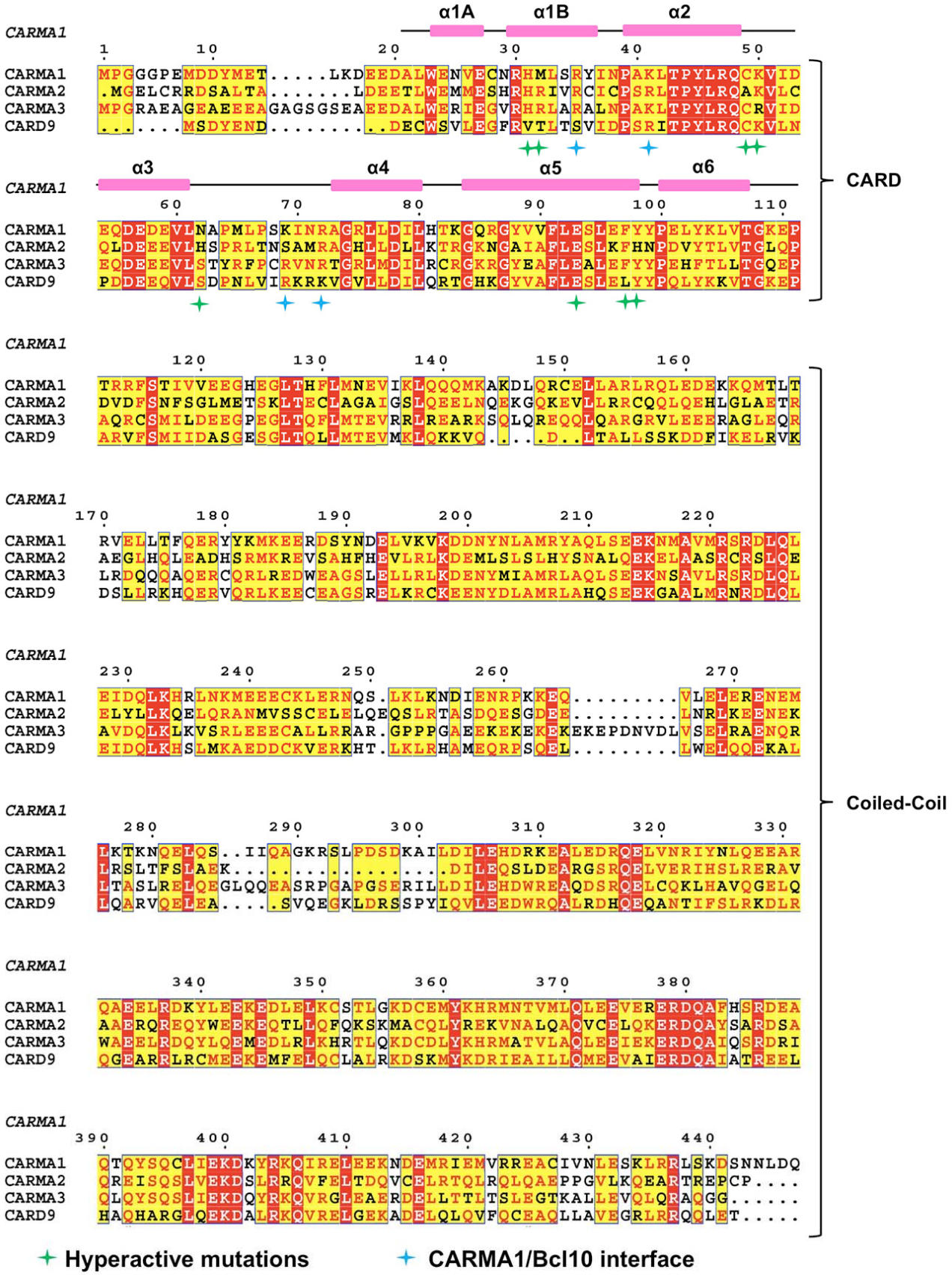

Figure S6. Sequence Alignment of CARMA1-3 and CARD9, Related to Figure 6. Residues that involved in Bcl10 interaction (cyan star) and hyperactive mutations (green star) are labeled.

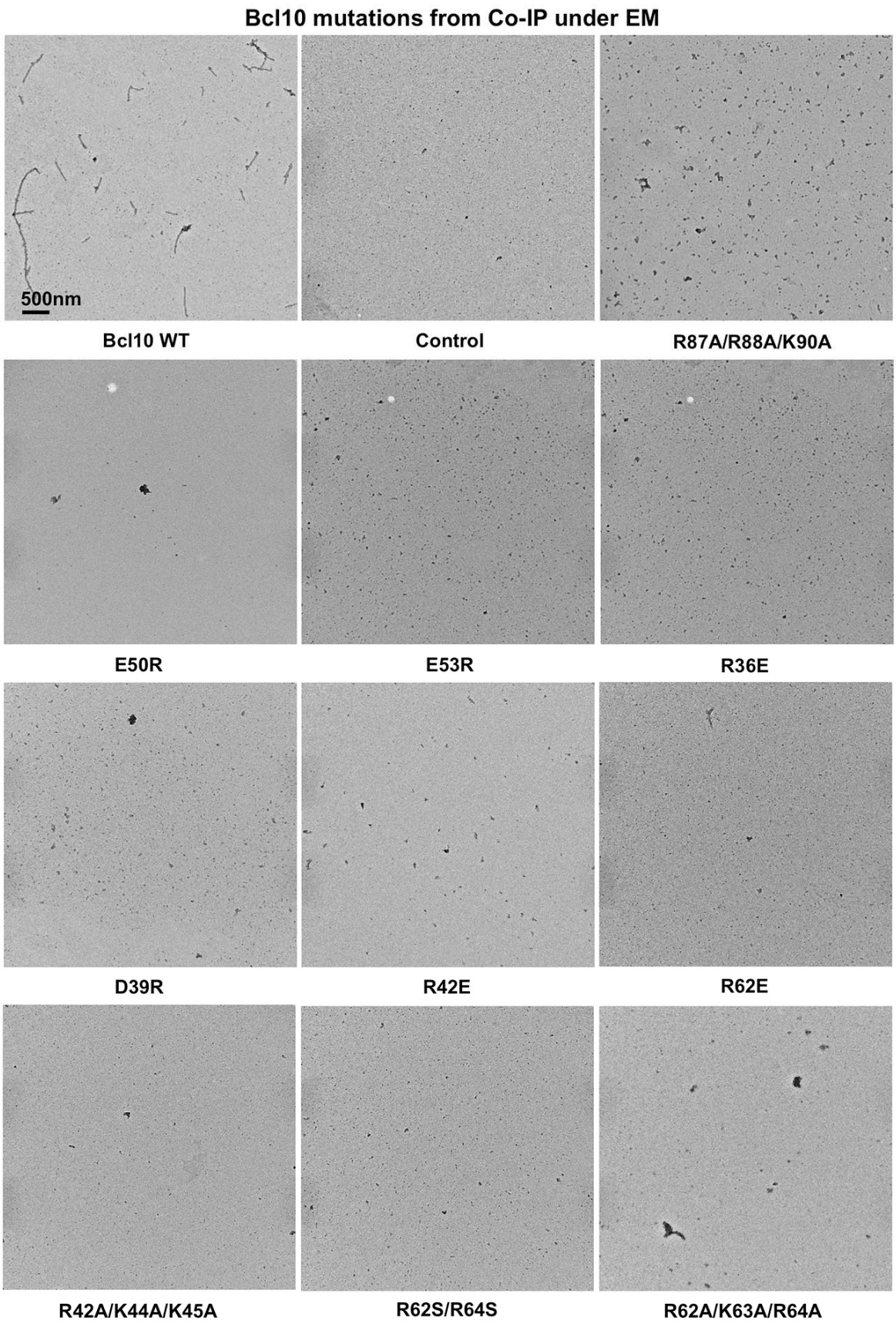

Figure S7. Structure-Based Bcl10 Mutagenesis *in Vitro* and in Cells, Related to Figure 7. EM images of immunoprecipitated overexpressed WT and mutant Bcl10 in 293T cells.

SUPPLEMENTAL TABLES

Table S1. Structural Statistics for the 10 Water Refined Structures of Bcl10 CARD, Related to Figure 4

NOE distance restraints	
All	1278
Intra-residue	693
Sequential (|*i-j*| = 1)	278
Medium range (2 ≤|*i-j*|≤4)	150
Long range (|*i-j*|> 4)	157
Dihedral angle restraints (derived from DANGLE)	222
RMSD from the mean coordinates (all atoms)	0.819
Number of distance violations > 0.5 Å	0.8
Ramachandran plot statistics	
Most favored regions	84.9%
Allowed regions	13.8%
Disallowed regions	1.3%

Table S2. Z-scores of Fitting of Different CARD Structures into the Bcl10 Filament Map, Related to Figure 4

CARD	Z-score of Fitting	Z-score of Fitting to the 3D-Map of the Opposite Hand
Bcl10	10.0	2.9
CARMA1	3.6	3.4
Apaf-1	1.7	2.0
ASC	1.8	2.1
RIG-I	4.0	2.1
cIAP1	1.8	2.9
Caspase-9	2.1	4.0
Nod1	1.8	2.4
Bcl10 α1-α5	1.9	2.4
Bcl10 w/ truncated α6	2.0	2.1

SUPPLEMENTAL EXPERIMENTAL PROCEDURES

Protein Expression and Purification

All constructs of CARMA1, Bcl10 and MALT1 are from human sequences. Various N-terminally His-tagged CARMA1 constructs were generated in vector pET28a. Full-length WT and C29A/C57A double mutant Bcl10 constructs with N-terminal MBP tag were generated in vector pDB-His-MBP. All mutagenesis experiments were performed using the QuikChange® Site-Directed Mutagenesis Kit (Stratagene). All proteins were expressed in *E. coli* BL21 (DE3) cells and purified by Ni-NTA resin (Qiagen) and gel filtration chromatography (Superdex 200 10/300 GL, GE Healthcare). Full-length MALT1 was engineered into vector pFastBacHTA with an N-terminal His-tag, expressed in insect cells, and purified similarly.

For co-expression of CARMA1 and Bcl10, N-terminally His-tagged CARMA1 constructs in pET28a were co-transformed into BL21 (DE3) cells with non-tagged Bcl10 (1-115) in vector pCDFDuet-1. The

CARMA1/Bcl10 complexes were purified by Ni-NTA affinity column in binding buffer containing 20 mM Tris at pH 7.5, 300 mM NaCl, 30 mM imidazole, 10 mM β-mercaptoethanol and 10 % glycerol followed by Superdex 200 gel filtration chromatography in buffer containing 20 mM Tris at pH 7.5, 150 mM NaCl and 5 mM DTT. For biotinylation, CARMA1 (8-172) was cloned into vector pDW363 fused with an N-terminal His-tag and a peptide substrate for *E. coli* biotin holoenzyme synthetase (BirA). The vector contains a coupled translation arrangement with BirA to allow enzymatic biotinylation of CARMA1 during expression (Tsao et al., 1996). The CARMA1 construct in pDW363 was co-transformed with non-tagged Bcl10 in pCDFDuet-1 to express the complex of biotinylated CARMA1 and Bcl10.

For ^{15}N and $^{13}C/^{15}N$ labeling, N-terminally His-tagged Bcl10 CARD (1-115) E53R mutant was transformed into BL21 (DE3) cells, which were then grown in a modified M9 minimal medium for uniform ^{15}N and/or ^{13}C labeling with ^{15}N NH_4Cl and/or [$^{13}C_6$]-glucose as the sole nitrogen and carbon sources, respectively (Marley et al., 2001). The proteins were purified with His-Pur™ Cobalt Resin (PIERCE). After removing the His-tag by overnight thrombin digestion at 4 ^{o}C, the protein sample was further purified by gel filtration with Superdex 200 10/300 GL (GE Healthcare).

Electron Microscopy

Copper grids coated with layers of plastic and thin carbon film were glow-charged before 5 µl of purified complexes were applied. Samples were left on the grids for 1 minute followed by negative staining with 5 % uranyl acetate for 1 minute and air dried. For limited proteolysis of immunopurified endogenous CBM signalosome, the samples were incubated with trypsin at 1:50 weight ratio for 1 hour before applying to the grids. *In vitro* reconstituted samples were imaged with a Tecnai F20 (FEI) transmission electron microscope (TEM) at the Rockefeller University operating at 120 keV with 60k magnification and micrographs were scanned at 1814 pix/inch using a Zeiss SCAI flat-bed densitometer (ZI/Carl Zeiss). Immunoprecipitated samples were imaged with a JEM-1400 TEM (JEOL, Ltd.) at Weill Cornell Medical College EM facility operating at 80 keV with 50k magnification on an Olympus-SIS Quemesa bottom-mount 11 megapixel digital camera. CARMA1 (8-302) and BCl10/CARMA1 (8-302) samples were imaged with JEOL 1200EX or Tecnai G^2 Spirit BioTWIN at Harvard Medical School EM facility operating at 80 keV.

For gold labeling of the biotinylated CARMA1/Bcl10 complex, 5 µl of the purified sample was applied to a copper grid and stand for 1 minute, followed by 3 washes with buffer containing PBS and 0.1 % BSA (Cat #: 25558, Electron Microscopy Sciences). The grid was then floated on 50 µl of 1:100 dilution of 10 nm streptavidin-gold solution (Cat #: 25269, Electron Microscopy Sciences) for 80 minutes and followed by 3 washes in PBS and 2 washes in water. The grid was fixed with 2.5 % glutaraldehyde in PBS for 3 minutes and washed with water twice. It was stained with 5 % uranyl acetate and examined using either a JEM-1400 (JEOL, Ltd.) or a Tecnai F20 (FEI) TEM.

For helical reconstruction, the CARMA1 (8-172)/Bcl10 (1-115) complex samples were applied to glow-discharged, carbon-coated grids, negatively stained using uranyl acetate (2 % w/v), and imaged in a Tecnai 12 (FEI) TEM at an accelerating voltage of 80 keV. Micrographs were scanned with a Nikon Coolscan 8000 at a raster of 4.16 Å per pixel. The helixboxer routine in EMAN (Ludtke et al., 1999) was used for cutting filaments from micrographs. The SPIDER software package (Frank et al., 1996) was used for most of the subsequent processing. From the EM images, 13,375 overlapping segments (100 px long) were collected, with a shift of 8 pixels between adjacent segments. The IHRSR algorithm (Egelman, 2000) was used for the three-dimensional reconstruction, starting with a solid cylinder as the initial reference. The resolution of the reconstruction was determined to be around ~20 Å by comparing with calculated maps of the fitted model at different resolutions.

Fluorescence Polarization Assays

Purified full length MBP-Bcl10 double mutant C29A/C57A was mixed with 5-fold molar excess of Alexa-488-C5-maleimide (Invitrogen) and incubated at room temperature for 2 hours. Gel filtration chromatography (Superdex 200, GE Healthcare) was used to remove free dyes. Fluorescence polarization assay was performed at 25 °C in buffer containing 20 mM Tris at pH 7.5, 150 mM NaCl, and 0.5 mM TCEP and in 20 µl volume. 2.5 µM (Figure 2A) and 4 µM (Figure 2C and 7A) labeled MBP-Bcl10 samples were used in CARMA1-induced Bcl10 polymerization experiments, and 6 µM was used in Bcl10 alone polymerization experiments (Figure 5F, 7C, and 7G). 4 µg TEV protease was added to

the samples right before the measurements for removal of the MBP tag to allow Bcl10 polymerization. For Hill coefficient measurements, we mixed 4 μg TEV protease with 20 μl WT Bcl10 in various concentrations with or without 0.1 μM CARMA1 (8-302), incubated at room temperature for 30min, and then at 4 °C overnight to finalize filament formation. 0.1 μM labeled Bcl10 was added before FP measurements, and ΔFP values within 60 min were plotted. Because under the low concentration of 0.1 μM Bcl10 does not form filaments by itself, we assumed that the FP increase was due to binding of labeled Bcl10 to pre-formed filaments, which renders the ΔFP a representation of the amount of pre-formed filaments in samples. Fluorescence polarization was measured using excitation/emission wavelengths of 495nm/519nm on a SpectraMax® M5e plate reader (Molecular Devices). Origin® was used in data processing and curve fitting.

CBM Signalosome Reconstitution

Purified 1.5 ml of 10 μM MBP-Bcl10 full length, 60 μl of 9.5 mg/ml TEV protease, 165 μl of 70 μM CARMA1 (8-172) and 45 μl of 230 μM full length MALT1 were mixed, incubated at room temperature on a rocker for 3 hours and purified by gel filtration chromatography.

MALT1 Paracaspase Activity Assay

MALT1 catalytic activity was monitored by the turnover of the fluorogenic tetrapeptide substrate Ac-LRSR-AMC (7-amino-4-methylcoumarin) (Rebeaud et al., 2008). Full length MALT1 alone or in the context of the CBM complex was mixed with Ac-LRSR-AMC (200 μM) in 20 μl reactions in buffer containing 20 mM Hepes at pH 7.5, 10 mM KCl, 1.5 mM $MgCl_2$, 1 mM EDTA, 1 mM DTT and 0.01 % Triton X-100. Fluorescence measurement upon substrate cleavage was performed with excitation/emission wavelengths of 360/465 nm at room temperature using SpectraMax® M5e plate reader (Molecular Devices) using 384-well black plates (Greiner). Reactions were monitored for up to 1 hour with 1 min intervals. Origin® was used in data processing and curve fitting.

Cell Transfection and Coimmunoprecipitation

293T cells were cultured in 90 % DMEM, 10 % FBS and penicillin G/streptomycin at 37 °C in a humidified atmosphere of 5 % CO_2 and transfected with 25 μg of pcDNA4-Flag-Bcl10 and 0.5 μg of pcDNA4-HA-CARMA1. At 24 hour after transfection cells were lysed in lysis buffer containing 20 mM Tris at pH 7.5, 150 mM NaCl, 10% glycerol, 10 mM β-mercaptoethanol and 1x protease inhibitors cocktail (Pierce) and briefly sonicated with 2-second pulses for three times. Cleared lysates were immunoprecipitated using anti-Flag agarose beads (Sigma). Bound complexes were eluted using 100 μg/ml 3x Flag peptide in lysis buffer. Western blot was performed with anti-HA and anti-Flag (Sigma) antibodies.

For immunoprecipitation of the endogenous CBM complex, 10^8 HBL-1 cells were resuspended in lysis buffer containing 25 mM Hepes at pH 7.5, 150 mM NaCl, 0.2 % NP-40, 10 % Glycerol, 1 mM DTT and protease inhibitor cocktail (Sigma) and incubated on ice for 10 min. Anti-Bcl10 polyclonal antibody (Santa Cruz Biotechnology) was biotinylated with EZ-Link NHS-PEG4-Biotin (Cat #: 21329, Thermo Scientific). Upon centrifugation to clear the lysate, the supernatant was mixed with biotinylated anti-Bcl10 and incubated overnight on a rocker at 4 °C. SoftLink soft release avidin resin (Promega, part # V201A) was used to immunoprecipitate the Bcl10-containing complex followed by elution with 5 mM Biotin in lysis buffer. Western blots were performed with anti-CARMA1 (Cell Signaling), anti-Bcl10 (DAKO) and anti-MALT1 (Cell Signaling) antibodies.

Crystallization and Structure Determination

The human CARMA1 CARD (residue 11-103) was crystallized by mixing 1 μl protein (10 mg/ml in 20 mM Tris at pH 8.0, 150 mM NaCl, and 5 mM DTT) with 1 μl of the reservoir solution containing 1.4 M $MgSO_4$ and 100 mM MES at pH 6.5 in a hanging drop vapor diffusion system at 20 ^oC. For phase determination, native crystals were soaked with 1 M potassium iodide (KI) for 1 minute. Native and KI-derivative crystals were briefly soaked into a cryo-solution containing 1.4 M $MgSO_4$, 100 mM MES at pH 6.5 and 20 % glycerol before saved in liquid nitrogen. All diffraction data were collected in house using R-AXIS IV. Data were processed with HKL2000 (Otwinowski and Minor, 1997). SHELXD

(Schneider and Sheldrick, 2002) was used to find the heavy-atom sites and the initial phases were determined by autoSHARP using single wavelength anomalous diffraction (Vonrhein et al., 2007). Model building was performed in program Coot (Emsley and Cowtan, 2004). Refinement was performed against the native data set using Phenix (Adams et al., 2010). Structural presentations were generated using Pymol (DeLano Scientific). The human CARMA1 CARD structure is highly similar to the recently published structure of mouse CARMA1 (Li et al., 2012). Structural homology was determined using DALI (Holm and Sander, 1995). Shape complementarity (sc) scores were calculated in CCP4 (Lawrence and Colman, 1993).

NMR Spectroscopy and Structure Calculations

All NMR experiments were recorded at 27 ^{o}C on Varian Unity Inova 600 MHz spectrometer equipped with cryoprobe. Sequential backbone assignment were achieved using two pairs of triple-resonance experiments [HNCA, HN(CO)CA, HNCO, HN(CA)CO, HNCACB and CBCA(CO)NH] with ^{15}N/^{13}C-labelled Bcl10 (1-115) E53R mutant in buffer containing 50 mM deuterated Arg/Glu at pH 6.5, 5 mM DTT, 0.02 % sodium azide and 7 % D_2O. Side-chain assignments were accomplished using HBHA (CO)NH, HCIH_COSY and HCIH_TOCSY. Distance restraints were derived from 3D ^{15}N-edited NOESY-HSQC (100 ms) and 3D ^{13}C-edited NOESY-HSQC (100 ms), 3D ^{15}N-edited side-chain only NOESY-HSQC (150 ms), and aromatic 2D NOESY-HSQC (200 ms). All spectra were processed with NMRPipe software package (Delaglio et al., 1995) and assigned with CCPNMR analysis (Vranken et al., 2005). Dihedral angle restraints were generated using DANGLE within CCPNMR. Initial structure calculation was performed on CcpNmr Grid Portal (Fogh et al., 2005; Nilges et al., 2008; Rieping et al., 2007; Vranken et al., 2005). The final structure calculation was performed using CNS (Brunger et al., 1998) with RECOORD script(Nederveen et al., 2005) starting from an extended conformation. Only residues 10-115 were included in the final round of calculation. A total of 1000 structures were calculated and ten lowest energy structures were refined in explicit water using CNS. The structures were analyzed within CcpNmr as well as using MolProbity (Chen et al., 2010). The dynamics of CARMA1 and Bcl10 CARDs was studied by measuring longitudinal (R1) and transverse (R2) relaxation rates using a series of ^{1}H-^{15}N-HSQC experiments (Kneller et al., 2002).

Luciferase Assays

CARMA1 and Bcl10 cDNAs were subcloned into the pcDNA4 plasmid by PCR with N-terminal HA tag on WT and mutant CARMA1 and N-terminal-Flag tag on WT and mutant Bcl10. 293T cells were plated at a density of 2×10^5 cells per well of a 12-well dish 24 hours before transfection. Reporter assays were performed by co-transfecting 250 ng of $(NF\text{-}\kappa B)_5$-Luc2CP-pGL4 and 25 ng of TK-Renilla internal control plasmid with indicated amounts of pcDNA4-Flag-Bcl10 and pcDNA-HA-CARMA1 plasmids or mutant Bcl10 or CARMA1 R35E/K69E using Lipofectamine 2000 (Invitrogen). Forty-eight hours after transfection, lysates were submitted to dual luciferase assays following manufacturer's protocol (Promega).

TRAF6 Knockdown

Predesigned siRNA targeting TRAF6 (ON-TARGETplus SMART pool L-004712-00; Thermo) and non-targeting control (ON-TARGETplus Non-targeting Pool D-001810-10) were electroporated in HBL-1 cells using the 96-well format Amaxa electroporator with 3 μM of siRNA using the SF transfection buffer (Amaxa). Cells were plated to a final concentration of 7.5 x 10^5 cells/ml in complete medium. At 48 hours after transfection cells were harvested and subjected to Western blotting, IP for BCL10 and complexes imaged using electron microscopy.

SUPPLEMENTAL REFERENCES

Adams, P.D., Afonine, P.V., Bunkoczi, G., Chen, V.B., Davis, I.W., Echols, N., Headd, J.J., Hung, L.W., Kapral, G.J., Grosse-Kunstleve, R.W., *et al.* (2010). PHENIX: a comprehensive Python-based system for macromolecular structure solution. Acta Crystallogr D Biol Crystallogr *66*, 213-221.

Brunger, A.T., Adams, P.D., Clore, G.M., DeLano, W.L., Gros, P., Grosse-Kunstleve, R.W., Jiang, J.S., Kuszewski, J., Nilges, M., Pannu, N.S.*, et al.* (1998). Crystallography & NMR system: A new software suite for macromolecular structure determination. Acta Crystallogr *D54*, 905-921.
Chen, V.B., Arendall, W.B., 3rd, Headd, J.J., Keedy, D.A., Immormino, R.M., Kapral, G.J., Murray, L.W., Richardson, J.S., and Richardson, D.C. (2010). MolProbity: all-atom structure validation for macromolecular crystallography. Acta Crystallogr D Biol Crystallogr *66*, 12-21.
Delaglio, F., Grzesiek, S., Vuister, G.W., Zhu, G., Pfeifer, J., and Bax, A. (1995). NMRPipe: a multidimensional spectral processing system based on UNIX pipes. J Biomol NMR *6*, 277-293.
Egelman, E.H. (2000). A robust algorithm for the reconstruction of helical filaments using single-particle methods. Ultramicroscopy *85*, 225-234.
Emsley, P., and Cowtan, K. (2004). Coot: model-building tools for molecular graphics. Acta Crystallogr D Biol Crystallogr *60*, 2126-2132.
Fogh, R.H., Boucher, W., Vranken, W.F., Pajon, A., Stevens, T.J., Bhat, T.N., Westbrook, J., Ionides, J.M., and Laue, E.D. (2005). A framework for scientific data modeling and automated software development. Bioinformatics *21*, 1678-1684.
Frank, J., Radermacher, M., Penczek, P., Zhu, J., Li, Y., Ladjadj, M., and Leith, A. (1996). SPIDER and WEB: processing and visualization of images in 3D electron microscopy and related fields. J Struct Biol *116*, 190-199.
Holm, L., and Sander, C. (1995). Dali: a network tool for protein structure comparison. Trends Biochem Sci *20*, 478-480.
Kneller, J.M., Lu, M., and Bracken, C. (2002). An effective method for the discrimination of motional anisotropy and chemical exchange. J Am Chem Soc *124*, 1852-1853.
Lawrence, M.C., and Colman, P.M. (1993). Shape complementarity at protein/protein interfaces. J Mol Biol *234*, 946-950.
Li, S., Yang, X., Shao, J., and Shen, Y. (2012). Structural Insights into the Assembly of CARMA1 and BCL10. PLoS One *7*, e42775.
Lin, S.C., Lo, Y.C., and Wu, H. (2010). Helical assembly in the MyD88-IRAK4-IRAK2 complex in TLR/IL-1R signalling. Nature *465*, 885-890.
Ludtke, S.J., Baldwin, P.R., and Chiu, W. (1999). EMAN: semiautomated software for high-resolution single-particle reconstructions. J Struct Biol *128*, 82-97.
Marley, J., Lu, M., and Bracken, C. (2001). A method for efficient isotopic labeling of recombinant proteins. J Biomol NMR *20*, 71-75.
Nederveen, A.J., Doreleijers, J.F., Vranken, W., Miller, Z., Spronk, C.A., Nabuurs, S.B., Guntert, P., Livny, M., Markley, J.L., Nilges, M.*, et al.* (2005). RECOORD: a recalculated coordinate database of 500+ proteins from the PDB using restraints from the BioMagResBank. Proteins *59*, 662-672.
Nilges, M., Bernard, A., Bardiaux, B., Malliavin, T., Habeck, M., and Rieping, W. (2008). Accurate NMR structures through minimization of an extended hybrid energy. Structure *16*, 1305-1312.
Otwinowski, Z., and Minor, W. (1997). Processing of X-ray diffraction data collected in oscillation mode. Methods Enzymol *276*, 307-326.
Rebeaud, F., Hailfinger, S., Posevitz-Fejfar, A., Tapernoux, M., Moser, R., Rueda, D., Gaide, O., Guzzardi, M., Iancu, E.M., Rufer, N.*, et al.* (2008). The proteolytic activity of the paracaspase MALT1 is key in T cell activation. Nat Immunol *9*, 272-281.
Rieping, W., Habeck, M., Bardiaux, B., Bernard, A., Malliavin, T.E., and Nilges, M. (2007). ARIA2: automated NOE assignment and data integration in NMR structure calculation. Bioinformatics *23*, 381-382.
Schneider, T.R., and Sheldrick, G.M. (2002). Substructure solution with SHELXD. Acta Crystallogr D Biol Crystallogr *58*, 1772-1779.
Tsao, K.L., DeBarbieri, B., Michel, H., and Waugh, D.S. (1996). A versatile plasmid expression vector for the production of biotinylated proteins by site-specific, enzymatic modification in Escherichia coli. Gene *169*, 59-64.
Vonrhein, C., Blanc, E., Roversi, P., and Bricogne, G. (2007). Automated structure solution with autoSHARP. Methods Mol Biol *364*, 215-230.

Vranken, W.F., Boucher, W., Stevens, T.J., Fogh, R.H., Pajon, A., Llinas, M., Ulrich, E.L., Markley, J.L., Ionides, J., and Laue, E.D. (2005). The CCPN data model for NMR spectroscopy: development of a software pipeline. Proteins *59*, 687-696.
Wolf, E., Kim, P.S., and Berger, B. (1997). MultiCoil: a program for predicting two- and three- stranded coiled coils. protein science *6*, 1179-1189.